Three-state cyclic voter model extended with Potts energy

György Szabó and Attila Szolnoki

Research Institute for Technical Physics and Materials Science, P. O. Box 49, H-1525 Budapest, Hungary

The cyclically dominated voter model on a square is extended by taking into consideration the variation of Potts energy during the nearest neighbor invasions. We have investigated the effect of surface tension on the self-organizing patterns maintained by the cyclic invasions. A geometrical analysis is also developed to study the three-color patterns. These investigations clearly indicate that in the ''voter model'' limit the pattern evolution is governed by the loop creation due to the overhanging during the interfacial roughening. Conversely, in the presence of surface tension the evolution is governed by spiral formation whose geometrical parameters depend on the strength of cyclic dominance.

I. INTRODUCTION

In systems with several species (particles, opinions, etc.) the cyclic invasion processes can maintain a self-organizing domain structure. Although this phenomenon is investigated extensively in different areas, such as the chemical reactions on crystal surfaces [1,2], biological (Lotka-Volterra) systems [3–6], Rock-Scissors-Paper (RSP) games in evolutionary game theories [7], and cyclically dominated voter models [8–10], the mechanism sustaining the polydomain patterns is not well understood. At the same time, this type of spatial self-organizations is believed to play crucial role in the biological evolution [11] and it can provide protection for the participants against some external invaders [12,13].

One of the simplest models exhibiting variations in a self-organizing domain structure was introduced by Tainaka and Itoh [8,9]. In this cyclically dominated voter model, three states (A, B, and C) are permitted on the sites of a square lattice. The system evolution is governed by the iteration of invasions between two randomly chosen nearest neighbors. The probability of each invasion process is independent of the location of neighboring sites and the invasion rates reflect cyclical (uniform) dominance. The strength of dominance was characterized by the difference of probabilities between two opposite invasions (e.g., $AB \rightarrow AA$ and $AB \rightarrow BB$). In the absence of cyclical dominance this system is equivalent to the voter model [15,16] exhibiting growing domains whose correlation length is proportional to $\sqrt{t}$ if the system is started from a random initial state. Contrary, for the spatial RSP game A beats B beats C beats A and these deterministic rules sustain a self-organizing, three-color polydomain structure in which the linear domain size can be characterized by a correlation length of $\xi \simeq 2.5$ (measured in lattice units). Tainaka and Itoh have shown that the typical domain size diverges when the cyclical dominance tends to zero [8]. Their numerical analysis is focused on the density of vortices that are defined by those points of a three-color map where the three states (domain walls) meet. In fact, one can distinguish vortices and antivortices (rotating clockwise and counterclockwise) and they are created and annihilated in pairs during the evolution of domain structure. According to the early Monte Carlo (MC) simulations the vortex density vanishes algebraically when decreasing the strength of cyclic dominance [8].

In the above system the domain walls separating two homogeneous domains are very irregular. This irregularity prevents the observation of expected spirals to be formed by the rotating vortex arms for smooth interfaces [9,14]. In the absence of cyclic invasion (and related vortex rotation) some features of the rough interfaces are already studied by several authors considering the two-state voter model [15–20]. In the presence of cyclic invasion, however, the topological and geometrical features of domain structure are not yet investigated rigorously even for smooth interfaces. Very recently some geometrical features and drift of a single spiral wave are studied by using a continuous reaction-diffusion model [21,22].

In the voter models the irregular interfaces are created by random invasions that are not influenced by the neighborhood. Smoother interfaces are observed for many other systems where the local change is directly affected by the neighborhood. The Potts models represent the simplest description of such a phenomenon. This is the reason why we have introduced a model where the nearest neighbor invasion is affected by an interfacial (Potts) energy [23,24] whose strength is controlled by an additional parameter. Investigating this model we can study the effect of surface tension on the self-organizing domain structures maintained by cyclic invasions on a square lattice. Performing systematic MC simulations we have determined the vortex density and interfacial energy in different stationary states. In order to have a deeper and more quantitative insight into the domain structure we have developed a method to study some geometrical features of the interfaces. This analysis throws light on some relevant geometrical features of the emerging domain structure and confirms the necessity of these types of sophisticated approaches.

II. THE MODEL

We consider a square lattice where at each site $\mathbf{x} = (i,j)$ (i and j are integers) there is a state variable with three possible states, namely, $s_x = 0,1,2$. The Potts energy for a configuration $s = \{s_x\}$ is defined as

$$H = - \sum_{\langle x, y \rangle} [\delta(s_x, s_y) - 1], \qquad (1)$$

where the summation runs over the nearest neighbor sites and $\delta(s, s')$ indicates the Kronecker's δ [23,24]. Notice that the coupling constant is chosen to be energy unit. In the present form the Potts energy measures the length of equivalent interfaces (in lattice unit $a=1$) separating the three types of domains and its inverse estimates the average domain radius [25]. Evidently, in the threefold degenerated (homogeneous) ground state $H=0$.

The configuration evolves in time according to elementary invasions between two nearest neighbor sites (**x** and **y**) chosen randomly. More precisely, a pair of neighboring state variables (s_x, s_y) (assuming $s_x \neq s_y$) transforms into (s_y, s_y) with a probability

$$\Gamma[(s_x, s_y) \rightarrow (s_y, s_y)] = \frac{1}{1 + \exp(K\Delta H + PD)}, \qquad (2)$$

where

$$\Delta H = H_f - H_i \qquad (3)$$

is the energy difference between the final and initial states, and K, as an inverse temperature, controls the effect of Potts energy on this single site flip. The second term in the argument of exponential function describes the cyclic dominance with a strength P, where

$$D = \begin{cases} +1 & \text{if } s_x = (s_y + 1) \mod 3, \\ -1 & \text{if } s_x = (s_y + 2) \mod 3. \end{cases} \qquad (4)$$

In the case $K=0$ the present model is equivalent to those introduced by Tainaka and Itoh [8]. Evidently, the ordinary three-state voter model is reproduced if $P=0$ and $K=0$. Furthermore, the limit $P \rightarrow \infty$ (for $|K| < P$) represents the deterministic RSP game. For $K > 0$, however, the interfaces become more smooth because the present dynamics suppresses those elementary processes that increase the interfacial (Potts) energy.

We have to emphasize that for $P=0$ this system exhibits domain growth independently of the value of K. Furthermore, in the present model the new state at a given site should be equivalent to one of the neigboring one. This means that the changes are localized along the boundaries separating the homogeneous domains.

Notice that the above rules conserve the cyclic symmetry among the three states. As a result, in a sufficiently large system the three states are present with the same probability (1/3). For small system, however, one of the species can become extinct due to the effect of fluctuations and finally the system evolves toward one of the three (homogeneous) absorbing states. Henceforth our analyses will be restricted to the large system limit that is provided by choosing the system size to be much larger than any length characteristic to the corresponding pattern.

The above model is investigated by MC simulations under periodic boundary conditions on a square lattice consisting
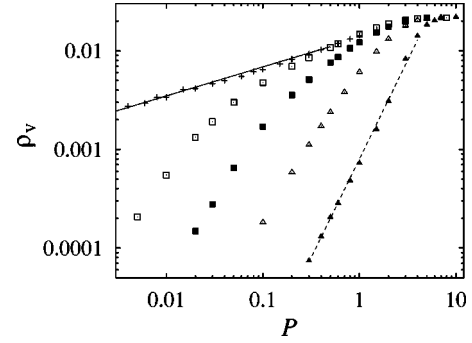

FIG. 1. Vortex densities as a function of P for $K=1$ (closed triangles), 1/4 (open triangles), 1/16 (closed squares), 1/64 (open squares), and 0 (pluses). The solid line shows the predicted power law behavior if $K=0$. The dashed line (with a slope of 2.05) indicates the best power law fit for $K=1$.

of $N=L \times L$ sites. The system is started from a random initial state where the three states are present with equal probabilities. During the simulations we have recorded the number of vortices and antivortices defined above. For this purpose we have counted those 2×2 block configurations containing all the three possible states [8–10]. After a suitable transition time we have determined the average vortex density as well as its fluctuation defined in Ref. [10]. The system size is varied from $L=400$ to 2000 to have sufficiently large number of vortices in the stationary states. The numerical results of vortex densities are summarized in a log-log plot as demonstrated in Fig. 1.

If $P \gg \max(K,1)$ then the dynamics is governed by the deterministic RSP rule that maintain a self-organizing state with small domain sizes ($\xi \simeq 2.5$) as mentioned above. Consequently the vortex density becomes independent of K for sufficiently large values of P as demonstrated in Fig. 1.

In the case $K=0$ the P dependence of vortex density can be well described by a power law, namely, $\rho_v \simeq P^\beta$ within the range $0.003 < P < 0.3$. The best fit is found for $\beta = 0.29(1)$ confirming our previous result [10]. At the same time Fig. 1 clearly demonstrates that the vortex density is dramatically reduced when the interfacial energy is switched on. For $K = 1$ the MC data can be well approximated by another power law with an exponent $\beta = 2.05(9)$. It should be emphasized that within the statistical error our data are consistent with a quadratic behavior. Similar behavior can be conjectured from the trends represented by MC data for lower K in Fig. 1. Unfortunately, we could not confirm this expectation by determining the leading term in the P dependence of vortex density for lower K values because this analysis requires extremely long run time and large sytems. Just to indicate the difficulties, the determination of a data point at low vortex densities has required more than four-week run time on a fast PC. We think that further numerical analyses are necessary to justify (or modify) the above conjecture.

Due to the long run times we could derive the vortex density fluctuations (χ) with an adequate accuracy. As demonstrated in Fig. 2, the numerical data indicate the divergence of the vortex density fluctuation in the absence of interfacial energy ($K=0$). Within the investigated region, this
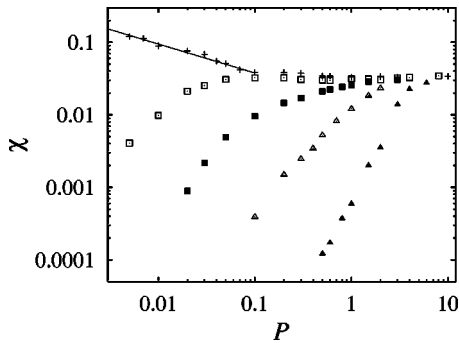
FIG. 2. Fluctuation of vortex density versus P for different K values denoted by the same symbols as in Fig. 1. The solid line indicates the fitted power law divergency in the absence of interfacial energy.

fluctuation can be approximated as $\chi \sim P^{-\gamma}$ with $\gamma = 0.3(1)$ in good agreement with a previous result [10].

In the presence of interfacial energy ($K > 0$) the vortex density fluctuation vanishes with P as indicated in Fig. 2. The vortex density fluctuation seems to be proportional to the vortex density for sufficiently low ρ_v. Similar features have been found for some systems of particles and antiparticles performing branching annihilating random walks [14,10]. This is the reason why we have reinvestigated a parallel drawn between the vortex dynamics in present model and a system of particles and antiparticles as suggested in Ref. [10]. According to a simple idea the rotating vortices form spirals whose long and narrow arms enhance the probability of the creation of a new vortex-antivortex pair. The movement of vortices can be well approximated by a random walk on a lattice. Furthermore, the vortex and antivortex annihilate each other when meeting at the same site during their random walks. The balance between the annihilation process and pair creation yields an average concentration in the stationary state. Within the framework of a simple mean-field analysis (details are given in Ref. [10]) the quadratic behavior of vortex density ($\rho_v \simeq P^2$) can be explained if we assume that the pair creation is proportional to $P\rho_v^{3/2}$ or $P^2 \rho_v$. From the view-point of vortex dynamics, however, both possibilities demand a better understanding about the relationship between the creation of vortex-antivortex pairs and the geometry of interfaces.

As mentioned above the total length of interfaces is equivalent to the Potts energy defined by Eq. (1). By this means we could easily determine the expected value of the interfacial energy per sites,

$$E = \frac{1}{N}\langle H \rangle, \qquad (5)$$

where $\langle \cdots \rangle$ indicates the average over the sampling time. The results of our simulations are summarized in a log-log plot (see Fig. 3).

At the first glance the P and K dependences of the vortex density and Potts energy seem to be very similar. However, the detailed numerical analysis gives different values for the
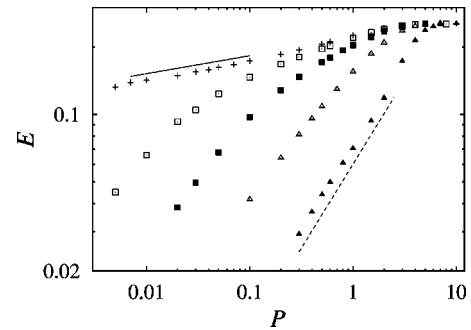

FIG. 3. Average Potts energy per sites as a function of P for the same values of K plotted in Fig. 1. The solid and dashed lines indicate the slopes of 0.08 ($K = 0$) and 1.3 ($K = 1$).

exponents when fitting a power law ($E = aP^\alpha$) for small P values. Namely, we have obtained $\alpha = 0.08(2)$ and 1.3(1) for $K = 0$ and 1, respectively.

If the convex domains are separated by approximately straight boundaries then $\beta = 2\alpha$ is expected as it is found for some other models [26]. The deviation from this behavior reflects the importance of curved interfaces due to vortex rotation.

The self-organizing domain structure shows striking differences depending on whether the interfacial energy is switched on or not. For the sake of illustration two typical patterns are shown in Figs. 4 and 5. In the absence of interfacial energy ($K = 0$) the nearest neighbor invasions yield irregular boundaries whose overhanging results in small islands (loops). Their random motion, extension, shrinking, splitting, and fission seem to play crucial roles in the pattern evolution as well as for the three-state voter model. In this former case ($P = 0$), however, these elementary events are not able to prevent the growth of domains whose characteristic linear size increases with time as $\sqrt{t}$ [19].

Choosing a particular initial state, it is already demonstrated that the cyclic dominance drives the vortex rotation (for $P > 0$) which is accompanied by spiral formation [9,10].
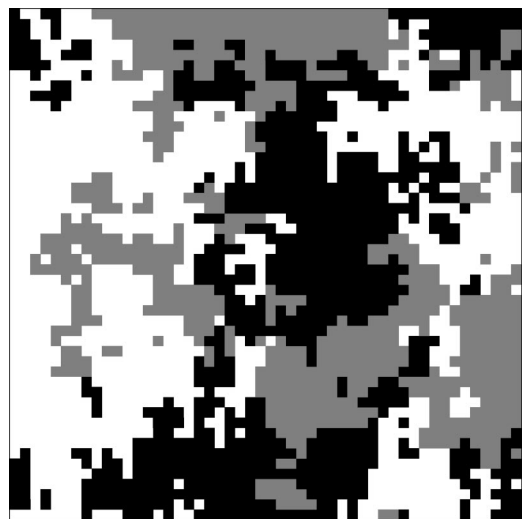

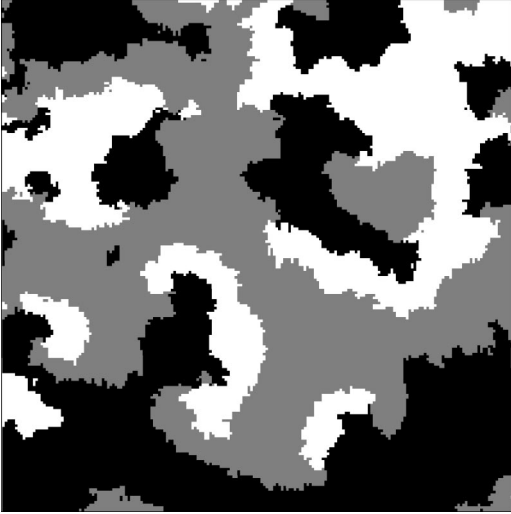FIG. 4. Typical part (50×50) of snapshot in a larger system for $K = 0$ and $P = 0.01$.

FIG. 5. Spiral formation sustained by the rotating vortices and antivortices is recognizable on a 200×200 part of a larger system for $K = 1/2$ and $P = 0.3$.

In Fig. 4 the rotating spirals are not recognizable due to the irregular interfaces. However, the spiral formation becomes visible when the interfacial roughness is reduced by the surface tension as demonstrated in Fig. 5.

In Fig. 5 one can easily identify the vortices and antivortices rotating clockwise and counterclockwise, respectively. This rotation creates spirals because the average invasion velocity is constant. We have to emphasize that this pattern cannot be characterized by a single length unit (e.g., correlation length) because the main features of spirals (armlength, average curvature, average distance, etc.) depend on the model parameters. This is the reason why we have developed a method to study some geometrical features of three-color maps on a square lattice.

III. GEOMETRICAL ANALYSES

On a three-color, continuous, planar map the domains are separated by three types of smooth boundaries. Dedicated points are the vertices where three or more boundaries meet. If such a map evolves smoothly then the appearance of vertices with more than three edges becomes negligible. Thus our analysis can be restricted to those maps that contain only three-edge vertices and antivortices. However, as we show later, the qualitative feature of the system remains unaffected if four-leg vertices are not ignored. One can easily check that these vortices and antivortices are positioned alternately along domain boundaries [10]. Our geometrical analysis will be focused on determining the average value of arclength, rotation of tangent vector, and curvature for those boundaries connecting a vortex and an antivortex. Henceforth the rotating vertex is called vortex.

On a square lattice the boundaries are polygons consisting of unit length parts whose tangential rotation may be $\Delta\phi = \pm\pi/2$ and 0. For a given vortex edge the tangential rotation is determined by summarizing these quantities step by step along the edge from a vortex to the connected antivortex. At the same time arclength is also obtained as the num-
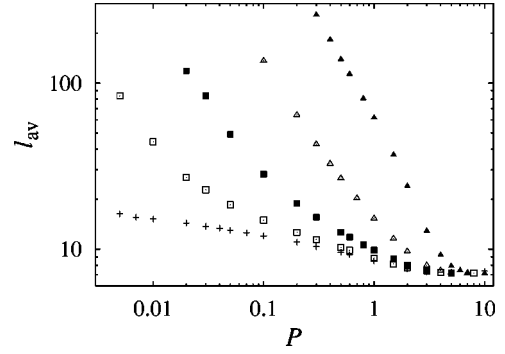

FIG. 6. Average arclength of vortex edges versus P for different K values. Symbols as in Fig. 1.

ber of steps. The elementary step is based on the identification of the 2×2 block configurations. This algorithm assumes that first we have determined the vortex positions. To reduce the statistical error this procedure was repeated many times during the simulations.

The above algorithm is well defined if the three-color pattern is free of four-edge vertices. Unfortunately, the investigated self-organizing patterns contain undesired four-edge vertices (see Figs. 4 and 5). Some of them (involving all the three states) can be considered as a vortex-antivortex pair just before their annihilation or after their creation [10]. The others involve only two states and make the paths (from vortex to antivortex) indefinite. Both types can be removed by executing an invasion through one of the randomly choosen four edges. Before the geometrical analysis all the investigated distributions are slightly adjusted by repeating the random invasions at the four-edge vertices until they vanish. Evidently, the effect of these modifications on the energy or vortex density is negligible if the typical domains are sufficiently large. The most relevant effect appears at $K = 0$ when the density of vortex-antivortex pairs is approximately $\rho_v/6$ in the whole region of P where we studied the system. Consequently, the P dependence of vortex density remains power law after the pattern adjustment.

After having removed the four-edge vertices the pattern becomes topologically equivalent to the continuous, three-color map mentioned above. In this case we can distinguish two types of boundaries, namely, loops (surrounding an isolated domain) and vortex edges (starting at a vortex and ending at one of the connected antivortices). Using the mentioned algorithm we have determined the average length l_{av} and tangential rotation ϕ_{av} of vortex edges.

In Fig. 6 the log-log plot of the average length of vortex edges shows that l_{av} increases slowly when P is decreased for $K = 0$. Significantly faster increase can be observed in the presence of surface tension. The arrangement of MC data for $K = 1$ has inspired us to fit a power law, $l_{av} = aP^{-\lambda}$ as we had done for the vortex density and the Potts energy per site. Within the same region of P the best fit is found for $\lambda = 1.75(5)$.

The above behavior is not surprising because the average vortex distance exhibits qualitatively similar P dependence. For the quantitative analysis an average vortex distance can be deduced from the density of vortices as $d_{av} = 1/\sqrt{\rho_v}$. The
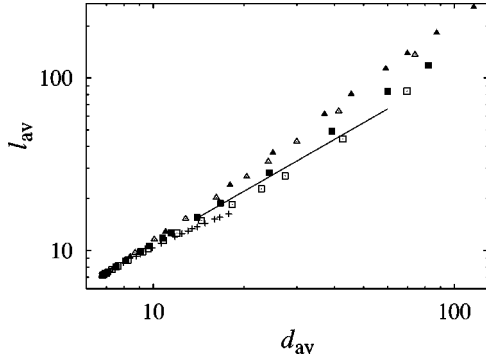
FIG. 7. Relation between the average vortex distance (d_{av}) and arclength of vortex edges (l_{av}) for those parameters (and symbols) plotted in Fig. 1. Both lengths are measured in units of lattice constant.

striking difference caused by the introduction of surface tension and cyclic invasion becomes visible when the pairs of data d_{av} and l_{av} are plotted on a log-log plot (see Fig. 7). In Fig. 7 the straight line ($l_{av} = 1.05 d_{av}$) demonstrates those sets of domain structures that can be well characterized by a single length scale. For example, such a situation can be observed when considering the domain growth in the three-state Potts model below the critical temperature. In the absence of interfacial energy the MC data indicate a significantly different relation that may be approximated as $l_{av} \simeq d_{av}^{0.8}$ within the given region. The slower increase of the average length of vortex edges can be explained by the increasing number of those vortex-antivortex pairs that have two common (short) edges. Shuch a pair is frequently created when the moving islands meet the third type of domain during their random movements.

An opposite tendency can be recognized for those cases where the spiral formation becomes relevant because the arclength of spiral arms always exceed the distance between the corresponding vortex and antivortex. At the same time our data reflect that the average tangential rotation of a vortex edge increases with d_{av}. This statement is supported by those data in Fig. 8 we obtained for $K>0$. Particularly, for $K=1$ one can observe that both ϕ_{av} (see Fig. 8) and l_{av} (Fig. 6) increases monotonously when P goes to zero. Unfortu-
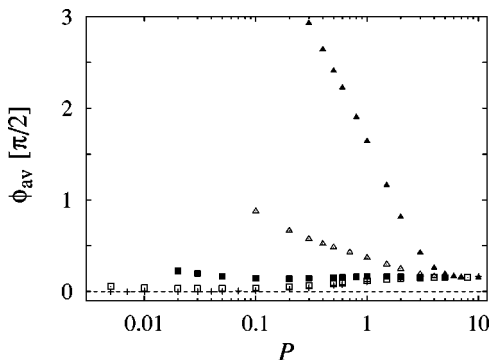

FIG. 8. Average tangential rotation of vortex edges as a function of cyclic dominance (P) for different K values (symbols as in Fig. 1).
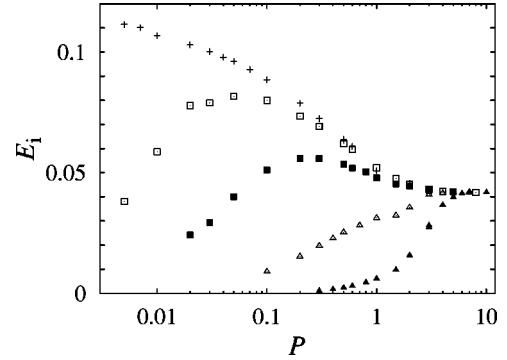
nately, we were not able to study what happens when the average tangential rotation becomes larger than 2π.

In Fig. 8 the angle of tangential rotation is measured in the unit $\pi/2$ that is a natural choice on a square lattice. One can observe that ϕ_{av} becomes practically zero in the $P \to 0$ limit in the absence of interfacial energy. In the light of this result one can think that the spiral formation does not play a dominant role in the pattern formation for $K=0$. At the same time, we should keep in mind that the cyclic invasion ($P>0$) is required to sustain the self-organizing domain structures, otherwise the domains would grow unlimited. Unfortunately, we cannot explain quantitatively the microscopic mechanism yielding this behavior. Now we can only give some additional arguments supporting the crucial role of islands as mentioned above.

The total interfacial (Potts) energy can be separated into two parts. The first contribution comes from the island boundaries and the second part from the vortex edges. Thus the energy per site can be written in the form

$$E = E_i + 3\rho_v l_{av}, \tag{6}$$

where E_i denotes the contributions of islands to the total Potts energy E defined by Eq. (5). The second term indicates that the contribution of vortex edges can be expressed as a product of the density of (three-edge) vortices (ρ_v) and the average length of vortex edges (l_{av}). Using this expression we can determine the values of E_i from those data plotted in Figs. 1, 3, and 6. The results of this calculation are illustrated in Fig. 9.

For $K=1$ the interfacial energy contribution of islands vanishes at sufficiently low values of P. This tendency can be observed in Fig. 9 for other $K>0$ values. The lower the value of K, the lower is the value of P where E_i becomes negligible. This means that in the stationary state the number of islands are reduced by the interfacial energy. This tendency can be visually checked if the reader compares the two snapshots shown in Figs. 4 and 5.

Notice, furthermore, that for $K=1$ the energy contribution of islands is negligible for weak cyclic dominance where the P dependence of E, ρ_v, and l_{av} can be well approximated by power laws as mentioned above. The substitution of the

FIG. 9. The interfacial energies of islands vs P for different K values. Symbols as in Fig. 1.

corresponding expressions into Eq. (6) yields a relation between the exponents, namely, $\alpha = \beta - \lambda$. Our numerical data support this result.

The investigation of E_i for $K=0$ shows surprising results. In the case of strong cyclic dominance the dominant part of interfacial energy comes from the vortex edges. According to our simulations, the contribution of E_i to the total interfacial energy increases, meanwhile E decrease (see Fig. 3) when decreasing P in the investigated region. Since $E > E_i$, therefore, these opposite tendencies imply the possibility of a break point for $P < 0.002$.

IV. CONCLUSIONS

We have numerically studied the effect of surface tension on the self-organizing patterns maintained by cyclic invasions among three species on a square lattice. For this purpose the cyclic voter model introduced by Tainaka and Itoh [8] is extended in a way that the cyclic symmetries are conserved. In the original model the invasion between two (randomly chosen) nearest naighbors is not affected by the neighborhood. In the extended model the nearest neighbor invasion rate is influenced by the neighborhood via taking the variation of Potts energy into account. Our analyses are restricted to those situations ($K \geq 0$) where this modification favors those invasions that reduce the length of interfaces separating the domains.

Our simulations have justified that the introduction of interfacial energy causes relevant changes in the observed patterns. To have a more quantitative and sophisticated picture we have determined the average value of some geometrical features of the interfaces (e.g., arclength and tangential rotation of vortex edges). This method is based on the analogy to the continuous limit of a three-color map. By this way we could study the contributions of vortex edges and islands separately. In the light of this analysis we can distinguish three types of typical domain structures.

In the deterministic limit $[P \gg \max(K,1)]$ the pattern consists of small compact domains and contains many vortices and antivortices. In the absence of interfacial energy ($K=0$) the typical domain size as well as the contribution of island interfacial energy increases when the the cyclic dominance (P) is decreased. Here the island creation via the interfacial roughening seems to be a relevant phenomenon. Conversely, in the presence of interfacial energy the islands vanish when P is decreased and vortex (spiral) rotations dominate the pattern evolution. The transitions among these typical behaviors are smooth.

Our numerical results are obtained in a limited region of the parameter P due to the technical difficulties appearing for large typical domain sizes. For some cases ($K=0$ and 1) our data can be approximated by power laws in a region of P. We are, however, not convinced that these (expected universal) behaviors remain valid for lower P values. For example, we do not know what happens when the average tangential rotation of vortex edges becomes significantly larger than 2π. Deviations can also appear for $K=0$ at lower P values where E_i is expected to decrease monotonously with P.

The suggested geometrical analyses confirm that the self-organizing patterns cannot be characterized by a single length unit as it happens for many other systems. In these cases two patterns cannot be transformed into each other by choosing a suitable length scale. In the presence of interfacial energy this feature is strongly related to the appearance of spiral vortex edges whose average tangential rotation remains unchanged during such a geometrical magnification. We think that this type of geometrical analysis unites different approaches and models, furthermore, it motivates a theoretical effort to find general relations among these quantities.

ACKNOWLEDGMENTS

[1] R.J. Field and M. Burger, *Oscillations and Traveling Waves in Chemical Systems* (Wiley Interscience, New York, 1985).

[2] M. Cross and P.C. Hohenberg, Rev. Mod. Phys. **65**, 851 (1993).

[3] J. Maynard Smith, *Evolution and Theory of Games* (Cambridge University Press, Cambridge, 1982).

[4] A.J. Lotka, Proc. Natl. Acad. Sci. U.S.A. **6**, 410 (1920); V. Volterra, *Leçon sur la Theorie Mathematique de la Lutte pour le Vie* (Gauthier-Villars, Paris, 1931).

[5] L. Frachebourg, P.L. Krapivsky, and E. Ben-Naim, Phys. Rev. E **54**, 6186 (1996).

[6] E. Ben-Naim, L. Frachebourg, and P.L. Krapivsky, Phys. Rev. E **53**, 3078 (1996).

[7] J. Hofbauer and K. Sigmund, *Evolutionary Games and Population Dynamics* (Cambridge University Press, Cambridge, England, 1998).

[8] K. Tainaka and Y. Itoh, Europhys. Lett. **15**, 399 (1991).

[9] K. Tainaka, Phys. Rev. E **50**, 3401 (1994).

[10] G. Szabó, M.A. Santos, and J.F.F. Mendes, Phys. Rev. E **60**, 3776 (1999).

[11] J. Maynard Smith, Nature (London) **280**, 445 (1979).

[12] M.C. Boerlist and P. Hogeweg, Physica D **48**, 17 (1991).

[13] G. Szabó and T. Czárán, Phys. Rev. E **63**, 061904 (2001).

[14] G. Szabó and M.A. Santos, Phys. Rev. E **59**, R2509 (1999).

[15] P. Clifford and A. Sudbury, Biometrika **60**, 581 (1973).

[16] R. Holley and T.M. Liggett, Ann. Prob. **3**, 643 (1975).

[17] J.T. Cox and D. Griffeath, Ann. Prob. **14**, 347 (1986).

[18] M.J. de Oliveira, J.F.F. Mendes, and M.A. Santos, J. Phys. A **26**, 2317 (1993).

[19] J.-M. Drouffe and C. Godrèche, J. Phys. A **32**, 249 (1999).

[20] I. Dornic, H. Chaté, J. Chave, and H. Hinrichsen, Phys. Rev. Lett. **87**, 045701 (2001).

[21] B. Sandstede and A. Scheel, Phys. Rev. Lett. **86**, 171 (2001).

[22] O-U. Kheowan, C-K. Chan, V.S. Zykov, O. Rangsiman, and S.

Müller, Phys. Rev. E **64**, 035201 (2001).

[23] R.B. Potts, Proc. Cambridge Philos. Soc. **49**, 106 (1952).

[24] F.Y. Wu, Rev. Mod. Phys. **54**, 235 (1982).

[25] O.G. Mouritsen, in *Kinetics of Ordering and Growth at Surfaces*, edited by M.G. Lagally (Plenum Press, New York, 1990).

[26] K. Binder and D. Stauffer, Phys. Rev. Lett. **33**, 1006 (1974); P.S. Sahni, G.S. Grest, M.P. Anderson, and D.J. Srolovitz, *ibid.* **50**, 263 (1983).